

Revisiting the thermal decomposition of five *ortho*-substituted phenyl azides by calorimetric techniques

Paolo Cardillo · Lucia Gigante · Angelo Lunghi ·
Paolo Zanirato

Received: 11 March 2009 / Accepted: 16 October 2009 / Published online: 6 November 2009
© Akadémiai Kiadó, Budapest, Hungary 2009

Abstract The thermal decomposition (TD) of 2-azidophenylmethanol (**1**), 2-azidobenzencarbaldehyde (**2**), 1-(2-azidophenyl)-1-ethanone (**3**), (2-azidophenyl)(phenyl)methanone (**4**) and 1-azido-2-nitrobenzene (**5**) was analysed by DSC, TG and C80 calorimetric techniques under both oxidative and non-oxidative conditions. The TD of these azides in solution is well known to give the corresponding benzoxazoles, generally in good yields, with the exception of azide **1**. When both the outcomes from the solid phase and in ‘solution phase’ TD reactions combined with the results from EI-MS experiments were considered, sufficient information was available to estimate the azides intrinsic molecular reactivity (MIR).

Keywords DSC · TGA-FTIR · C80 techniques · Heat flux calorimetry · Kinetic and thermodynamic parameters · MS (EI) spectroscopy · Pericyclic reactions and mechanism · Phenyl azides · Thermal decomposition in ‘solution phase’ and ‘solid phase’

Introduction

Organic azides are a well-studied class of compounds that are easily prepared and transformed into a variety of functional groups (amines, triazenes, aza-ylides and isocyanates), reactive intermediates (nitrenes, nitrenium ions)

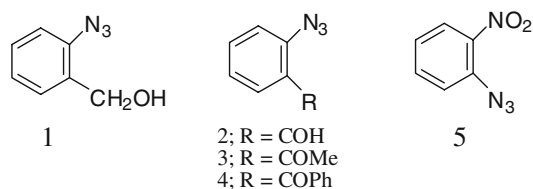
and nitrogen-containing heterocycles (azirines, aziridines, triazoles, triazolines and azoles). Azides have several defence and industrial applications, including use as propellants, explosives, polymer cross linkers, rubber vulcanisation agents, reactive dyes and blowing agents, and are also found in biologically and pharmaceutically active compounds [1–3]. Although most chemists recognise that organic azides have extremely useful applications in modern organic chemistry, very few reports mention their potentially dangerous properties [4]. However, an overwhelming interest in the explosive properties of metal azides [5] and poly-azide organic compounds [6] has developed during the last decade.

Compounds containing one (or more) azido groups, especially in conjunction with other ‘explosophores’, are known for their treacherous sensitivity to heat and/or shock [4, 6–8]. Despite the apparent lack of shock sensitivity warnings on its MSDS, the 4-azidobenzaldehyde is too shock sensitive to be isolated in other than very small quantities [9]. It is often prudent to perform thermal analyses of such compounds using a differential scanning calorimeter (DSC) and/or a thermal gravimeter (TG), as well as C80 calorimetric analysis. Papers discussing the most likely thermal decomposition (TD) hazards of aryl [10] and heteroaryl [11, 12] azides have recently been published.

In contrast, the TD of simple organic azides under ‘controlled’ conditions is a synthetically fruitful reaction that gives rise to a great variety of products. The outcomes of TD reactions are generally dependent upon the medium, as well as the substrate and its substituent(s). These factors may direct the reaction’s mechanism toward a concerted extrusion of nitrogen or toward the formation of a ‘free’ nitrene [13]. The intermediate nitrene can exist in either a singlet or triplet (S or T) electronic ground state, where the former is normally favoured by conjugated electron

P. Cardillo (✉) · L. Gigante · A. Lunghi
Stazione Sperimentale per i Combustibili SSC,
Viale A. De Gasperi 3, 20097 San Donato Milanese, MI, Italy
e-mail: cardillo@ssc.it

P. Zanirato
Dip.to di Chimica Organica ‘A. Mangini’, Viale Risorgimento 4,
40136 Bologna, Italy



Scheme 1 *o*-Phenyl azides used in this study

withdrawing groups and the latter is typically favoured by electron-donating groups on the phenyl azide [14–18].

The aim of this study is to disclose the hazardous nature, if any [6–9], of 2-azidophenylmethanol (**1**) and the *o*-oxophenylazides: 2-azidobenzene-carbaldehyde (**2**), 1-(2-azidophenyl)-1-ethanone (**3**), (2-azidophenyl)(phenyl)methanone (**4**) and 1-azido-2-nitrobenzene (**5**) (Scheme 1). The kinetic and thermodynamic studies of the ‘controlled’ TD reactions of the compounds **2–5** in solution have been previously reported [19–21]. These compounds were also selected for study because re-examining their TD reactions should shed further light on their relevance in the long debated electrocyclic mechanism of benzoxazole formation. These studies were performed using advanced calorimetric and thermo-analytical methods (DSC, TG and C80) under both oxidative and non-oxidative conditions, which were coupled to analyses of the gasses emitted by TGA- and C80-FTIR. In contrast, azide **1** was selected as a comparative probe to assess the energy required for (presumably) non-concerted TD processes.

In order to predict and detect the early stage processes involved in the TDs of azides **1–5**, both theoretical calculations using the CHETAH (CHEMical Thermodynamic and Hazard Evaluation) software package and electron impact mass spectroscopy (EI-MS, 70 eV) were performed.

Experimental section

Materials and chemicals

The phenyl azides (**1–5**) used in this study were prepared as follows: 2-Azidophenylmethanol (**1**), 1-(2-azidophenyl)-1-ethanone (**3**), (2-azidophenyl)(phenyl)methanone (**4**) and 1-azido-2-nitrobenzene (**5**) were prepared according to the standard procedure of Noeltling and Michel [22] with some modifications to improve safety [23]. The desired azides were prepared by diazotization of the corresponding amines, obtained from Sigma–Aldrich of Italy, and subsequent treatment of the resulting diazonium salt solutions with a sodium acetate-buffered aqueous solution of sodium azide. Alternatively, 2-azidobenzene-carbaldehyde (**2**) was prepared by the oxidation of azide **1** with pyridinium chlorochromate according to the previously described protocol (mp 36–37 °C) [24].

The isolated solid organic azides **1–5** were handled using standard techniques, while their purification and characterisation were carried out by standard methods [25–29]. The IR, ¹H-NMR and mass spectroscopic data obtained for azides **1–5** are consistent with their assigned chemical structures. Chromatographic filtration was carried out on ‘Florisil’ BDH, 60–100 mesh, using petroleum ether (distillation range 30–60 °C) as the eluent: (**1**, mp 52–53 °C [25]; **2**, mp 34–36 °C [26]; **3**, mp 22–23 °C (bp. 121 °C/17 mm) [27]; **4**, mp 36–37 °C [28]; **5**, mp 51–53 °C [29].

Physical measurements and experimental conditions

Spectral characterisation of azides **1–5** [30]

The IR spectra of azides **1–5** were measured as neat films using a Perkin-Elmer Spectrum 2000 FT-IR spectrometer. ¹H-NMR and ¹³C-NMR spectra for all five compounds were recorded on a Varian Gemini 300 and agree with the data reported in the literature [31–35].

Mass spectra were recorded on VG7070E instruments using an electron impact ionisation method (70 eV) at the same pressure (10^{−7} atm) and temperature (27 °C). The melting points of azides **1–5** were devised from the endothermic melting peak in the DSC’s thermal plot and were in agreement with the previously reported values [24–29].

Thermal performances were measured relative to a reference sample in the DSC 820 and 823e Mettler Toledo instruments with the following accuracy standards: (i) 5 °C min^{−1} for the evaluation of decomposition enthalpy under both oxidative and closed steel vessel non-oxidative conditions from 30 to 300 °C; (ii) 2, 5, 10 and 15 °C min^{−1} for the evaluation of kinetic data from dynamic heating under a nitrogen atmosphere in a closed glass vessel from 30 to 300 °C, unless otherwise stated [36]. The best measurements of self-heating rates were obtained using a C80 Setaram calorimeter from 30 to 300 °C, to a scan rate (Φ) of 0.3 °C min^{−1} unless otherwise stated.

The thermogravimetric analysis, which measures weight loss under both oxidative and non-oxidative heating conditions and which takes place in an open vessel, allows the IR and mass spectra (MS) of the released gases to be recorded. The instruments used in the apparatus were a TG/DSC 1 Star system from Mettler Toledo, a Nexus TGA FTIR with a Nicolet interface and a Pfeifer Vacuum Thermostar MS spectrometer.

Results and discussion

Thermodynamic values for azides **1–5** (heats of formation/ $\Delta_f H$, combustion/ $\Delta_c H$, and decomposition/ $\Delta_d H$) were

calculated using the CHETAH software package (ASTM Computer Program for Chemical Thermodynamic and Energy Release Evaluation, CHETAH, ver. 8.0; 2005) and are listed in Table 1. The heats of decomposition were predicted to be from -5.21 to -3.30 kJ g^{-1} . For reference, when a compound's $\Delta_d H$ value is over the threshold of -2.93 kJ g^{-1} , it is considered to be dangerous.

The data predicted by the upgraded version of CHETAH, although approximate [37], are very useful [38] for the characterisation and comparison of substances belonging to the same class [39]. In this case, the combined software calculated total risk value, called ERP (Energy Release Potential), appears to be high (Fig. 1).

The use of DSC, TG-DTA and Setaram C80 FTIR calorimetry techniques enabled us to characterise the (in)stability of azides **1–5** by determining their physical parameters (pressure/ P , temperature/ T_n , decomposition rate/ k and energetic parameters (activation energy/ E_a , enthalpy/ ΔH and entropy/ ΔS of decomposition). The experimental heats of decomposition/ kJ g^{-1} obtained by DSC analysis, as well as the related initial/ T_i and peak/ T_p temperature/ $^{\circ}\text{C}$, are shown in Table 2.

The DSC data for the TD of oxoazides **2–5** show similar behaviour. They were insensitive to atmospheric conditions, while azide **1**'s behaviour was strongly affected by the closed- or open-vessel conditions. The absolute values of heat capacity measured for compounds **2–5** under

Table 1 Heats of formation/ $\Delta_f H$, combustion/ $\Delta_c H$, and decomposition/ $\Delta_d H$ for azides **1–5** calculated with CHETAH

	1	2	3	4	5
$\Delta_f H/\text{kJ mol}^{-1}$	202.84	266.32	215.95	364.03	370.91
$\Delta_c H/\text{kJ g}^{-1}$	-25.5	-24.64	-26.13	-29.42	-19.59
$\Delta_d H/\text{max}/\text{kJ g}^{-1}$	-3.61	-3.83	-3.42	-3.3	-5.21

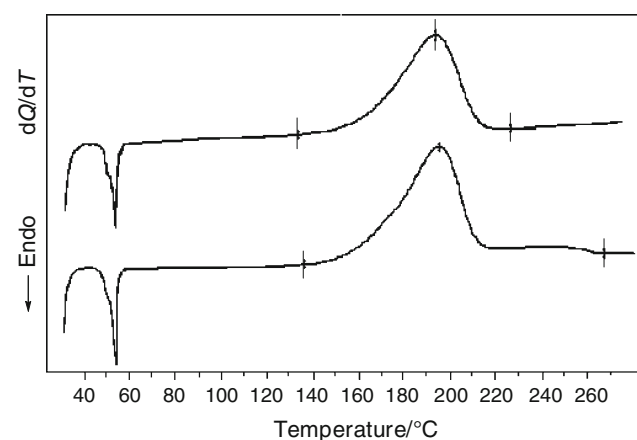


Fig. 1 DSC profiles of the TD of the azide **1** performed at heating scan rate $\Phi = 5$ $^{\circ}\text{C min}^{-1}$ under nitrogen (upper) and in static air (lower)

Table 2 DSC^{a,b} and C80^c determined heats of decomposition/ J g^{-1} and temperature/ $^{\circ}\text{C}$ for the thermal decompositions (TD) azides **1–5** under various conditions

	$\Delta_d H_{\text{air}}^a$	$\Delta_d H^b$	$\Delta_d H^c$	T_i^d	T_p^e	T_i^f	T_p^g
1	-1928.53	-1563.42	-1809.13	135.21	194.71	116.6	162.8
2	-708.85	-709.03	-680.9	113.06	159.49	91.97	127.86
3	-462.43	-464.35	-394.54	82.16	130.83	58.57	101.69
4	-374.02	-377.53	-381.72	89.57	138.7	77.72	120.55
5	-527.13	-576.9	-471.5	71.34	119.81	119.81	92.6

^a DSC data refers to different heating scan rate $\Phi = 5$ $^{\circ}\text{C min}^{-1}$ in static air

^b Under nitrogen

^c C80 data refers to a scan rate $\Phi = 0.3$ $^{\circ}\text{C min}^{-1}$ in a closed-vessel under nitrogen

^d Initial decomposition temperature in static air

^e Peak temperature in static air

^f Initial decomposition temperature under nitrogen

^g Peak temperature under nitrogen

nitrogen ($\Delta_d H$) were comparable, or slightly larger in the case of the more oxygenated azide **5**, with those measured in static air ($\Delta_d H_{\text{air}}$), which confirms a concerted pathway. In contrast, under nitrogen and in a closed vessel only azide **1** exhibited a significant decrease in ($\Delta_d H$) such that ($\Delta_d H_{\text{air}}$) \gg ($\Delta_d H$). As expected the individual TD C80 FTIR profile for compound **1**, measured at various heating rates, displays an endothermic melting peak at 53 $^{\circ}\text{C}$, corresponding to the solid to liquid transition, which is followed by a single exothermic peak starting at a T_i of 116.6 $^{\circ}\text{C}$, and characterised by a T_p of 162.8 $^{\circ}\text{C}$ with a decomposition enthalpy ($\Delta_d H$) of -1809.13 J g^{-1} and pressure increase (ΔP) of 8 bar (Fig. 2).

Interestingly, azides **2–5** show DSC and C80 FTIR profiles containing a second exothermic peak that corresponds to the decomposition of the initial cyclisation products **2a–5a**. In the instance of the azide **4**, a third peak,

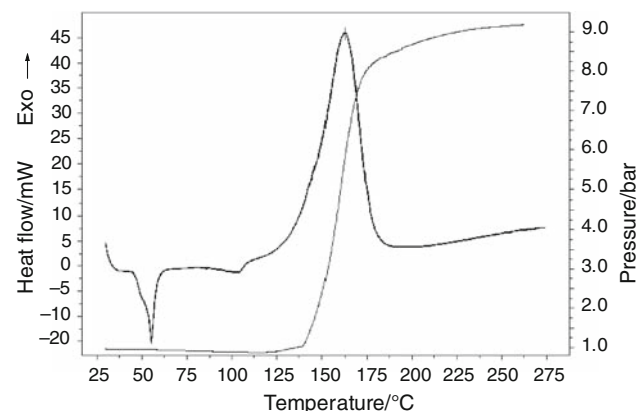
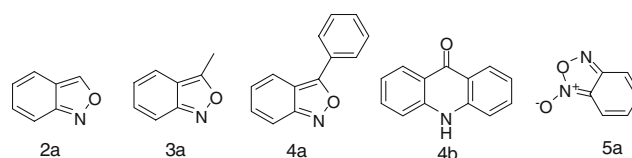


Fig. 2 C80 plot of the TD in glass vessel at scan rate $\Phi = 0.3$ $^{\circ}\text{C min}^{-1}$ under nitrogen of the azide **1**

4b, was also detected (see Figs. 3, 4 for the TD of compound **4**).

According to the previously reported results from ‘controlled’ TDs in inert solvent, we expected that the second (and third) exothermic peaks would correspond to the cyclised compounds namely: benzo[*c*]isoxazole **2a** [19, 20], 3-methylbenzo[*c*]isoxazole **3a** [19, 20], 3-phenylbenzo[*c*]isoxazole **4a**, acridin-9(10H)-one **4b** [19–21] and benzo[*c*][1,2,5]oxadiazole 1-oxide **5a** [19, 20] (see Scheme 2). The formation of these cyclisation products accounts for the lower decomposition enthalpy ($\Delta_d H$) observed for azides **2–5**, relative to azide **1**, since part of the heat is devolved to the cyclisation process.

The structures of **2a–5a** and **4b** were confirmed by coupled TG-SDTA-FTIR-MS analysis of the gases evolved during the TD reactions, and by analysis of ^1H - and



Scheme 2 Main products detected from TD of the *o*-phenyl azides **2–5**

^{13}C -NMR spectra of the final residues resulting from azides **3** and **4**.

Table 3 reports the experimental values for the heat of decomposition/ J g^{-1} and the associated temperatures, initial/ T_i and peak/ T_p , for the cyclisation products.

The failure of the *o*-carbinol group to assist the pericyclic mechanism is significant and can be seen by comparing the Arrhenius activation energy (E_a) for azides **1**, **3** and **4**. The E_a parameter can be used to calculate enthalpies [$E_a = \Delta H^\ddagger + RT$] and entropies (ΔS_a) of activation. The DSC profiles (see Fig. 5 for the DSC profile of azide **1**) were measured at different heating rates (four DSC runs at 2, 5, 10 and 15 $^\circ\text{C min}^{-1}$) and were analysed using the standard ASTM E698 method for reactions whose behaviour is well described by the Arrhenius equation. Figure 5 shows a plot of $\log b$ ($b =$ heating rate in K/min) versus $1/\text{K}$, which allows the apparent activation energy (E_a), the pre-exponential factor (A^0) and the kinetic constant k at each absolute temperature to be calculated.

The TD curves at various temperatures ranging from 90 to 200 $^\circ\text{C}$ for azides **1**, **3** and **4** were fit to first-order kinetics as plots of $\ln(k/\text{min}^{-1})$ versus T/K and displayed a linear trend with correlation coefficients of greater than 0.999. The activation energies (E_a) of these azides were calculated, along with the corresponding frequency factor $\ln(A^0/\text{min}^{-1})$ values. Assuming unimolecular processes, we then calculated the activation enthalpies ($\Delta_a H^\ddagger$) and

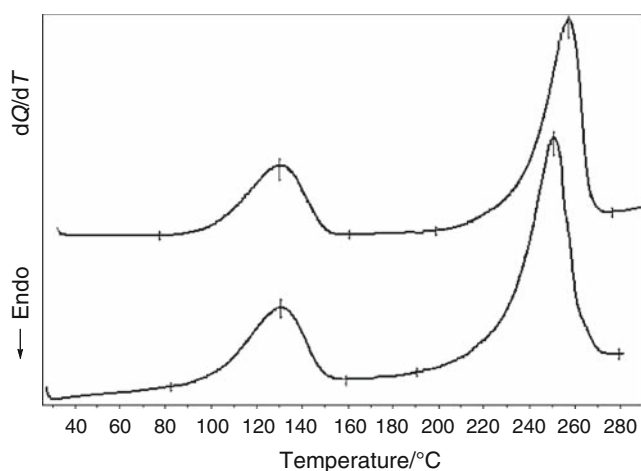


Fig. 3 DSC profiles of the TD of the azide **3** performed at heating scan rate $\Phi = 5$ $^\circ\text{C min}^{-1}$ under nitrogen (upper) and in static air (lower)

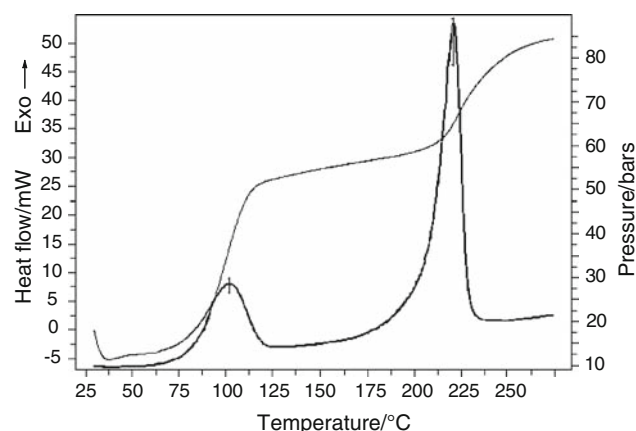


Fig. 4 C80 plot of the TD in glass-vessel at heating scan rate $\Phi = 0.3$ $^\circ\text{C min}^{-1}$ under nitrogen of the azide **3**

Table 3 DSC^{a,b} and C80^c determined heats of decomposition/ J g^{-1} and thermal decomposition temperature/ $^\circ\text{C}$ for the products formed by intramolecular cyclisation **2a–5a** and **4b** from **2–5**

	$\Delta_d H_{\text{air}}^a$	$\Delta_d H^b$	$\Delta_d H^c$	T_i^d	T_p^e
2a	−932.21	−953.99	−1054.59	152.26	189.36
3a	−1086.69	−904.9	−1137.66	164.24	220.96
4a	−60.45	−41.24	−54.29	143.26	149.06
4b	−488.3	−612.01	−825.83	190.76	245.66
5a	−1846.64	−1835.67	−1953.91	126.95	193.42

^a DSC data refers to different heating scan rate $\Phi = 5$ $^\circ\text{C min}^{-1}$ in static air

^b Under nitrogen

^c C80 data refers to heating scan rate $\Phi = 0.3$ $^\circ\text{C min}^{-1}$ in a closed-vessel under nitrogen

^d Initial decomposition temperature under nitrogen

^e Peak decomposition temperature under nitrogen

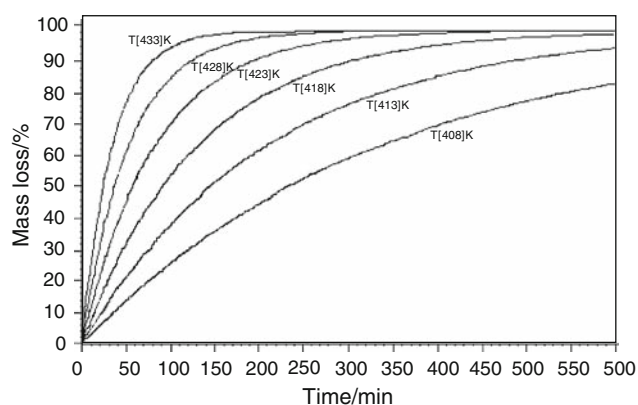


Fig. 5 C80, TD curves of the azide **1**; mass loss/% versus times/min at various temperatures/K

entropies (S_a) from the data (see Table 4), which we compared to those reported for ‘controlled’ decompositions (Table 5).

The ASTM calculated half-life ($t_{1/2}$) for the TD of azide **1** at 25 °C (Table 4) was about thousand times slower than that of azides **3** and **4** (the latter two being comparable), and the corresponding activation energies (E_a) were 134.3 versus 105.3 and 105.3 kJ mol⁻¹, respectively. Unfortunately, no kinetic or energetic data concerning azide **1** under ‘controlled’ thermal conditions has been reported, but the activation energies (E_a) calculated for azides **3** and

Table 4 Kinetic parameters and activation energies for the TD of azides **1**, **3** and **4** calculated from thermo-analytic data obtained using the ASTM E698 method

	k^a/min^{-1}	$\ln A^\circ$	$E_a^d/\text{kJ mol}^{-1}$	$\Delta_r H^\ddagger/\text{kJ mol}^{-1}$	$S_a^e/\text{J K}^{-1} \text{mol}^{-1}$
1	2.19×10^{-11}	29.65	134.3	131.8	-0.7
3	2.12×10^{-8}	24.83	105.3	102.8	-40.3
4	2.12×10^{-8}	24.84	105.3	102.8	-40.4

DSC data refer to four runs at heating scan rate $\Phi = 2, 5, 10$ and 15 °C min⁻¹ in static air

^a Calculated at 298 K

Table 5 Kinetic parameters and activation energies calculated from data involving ‘controlled’ TDs of azides **1**, **3** and **4**

	k/min^{-1}	$\ln A^\circ$	$E_a^d/\text{kJ mol}^{-1}$	$\Delta_r H^\ddagger/\text{kJ mol}^{-1}$	$S_a^e/\text{J K}^{-1} \text{mol}^{-1}$
1 ^{a,b}	4.5×10^{-4}	-	-	-	-
3 ^a	8.20×10^{-7}	27.1	107.9	105.4	-35.6
4 ^c	9.25×10^{-7}	28.8	102.7	99.6	-57.6

Obtained in decalin solutions

^a From [19]

^b Measured at 161.6 °C

^c Data from [21]

4 under ‘controlled’ thermal conditions were lower than observed for azide **1** and were comparable at 107.9 and 102.7 kJ mol⁻¹, respectively [19, 21]. This implies considerable anchimeric assistance via the phenyl ring, instead of an intermediate free nitrene, in the quick extrusion of nitrogen from **3** and **4** in route to the formation of the corresponding benzoisoxazoles **3a** and **4a**. This peculiar trend is also confirmed by the negative activation entropies ($\Delta_a S$) calculated for the TD of aryl azides **3** and **4** under both conditions (see Tables 4, 5).

The C80 analysis of azide **4** (see Fig. 6) detected at least three exothermic processes, with $T_p = 120.45, 149.06$ and 245.66 °C, and with $\Delta_a H = -381.72, -54.29$ and -825.83 J g^{-1} , respectively.

The C80 analysis of azide **4**s TD is characterised by an overall pressure increase of about 6 bars with the change during the first decomposition, which presumably corresponds to the extrusion of nitrogen. A second pressure increase, which can be ascribed to the loss of carbon monoxide from benzoisoxazole **4a**, rather than the loss of a residual nitrogen, suggests the possible initial formation of a bridged bicyclic compound resulting from an intramolecular 1,3-dipolar addition [21], but can be ruled out in this case. It is well known that at high temperatures **4a** isomerises to acridinone **4b** [28], and the TD behaviour of *o*-(2-azidophenyl)(phenyl)methanone (**4**) should not be considered fundamentally different. In light of the reported thermodynamic studies [40] of acridinone **4b**, the exothermic enthalpy peak of -825.8 J g^{-1} appears to result from the conversion of **4a** to **4b**, which can be detected by ¹H-NMR, along with small amounts of various other products (*N,N*-diphenylamine, 2-aminobenzaldehyde and carbazole) that are detected by TG-FTIR.

The thermal behaviours of azides **1–5** were analysed by EI-MS (70 eV) under the ion chamber conditions at 27 °C and a pressure of 10⁻⁷ atm. In the case of azide **4**, the

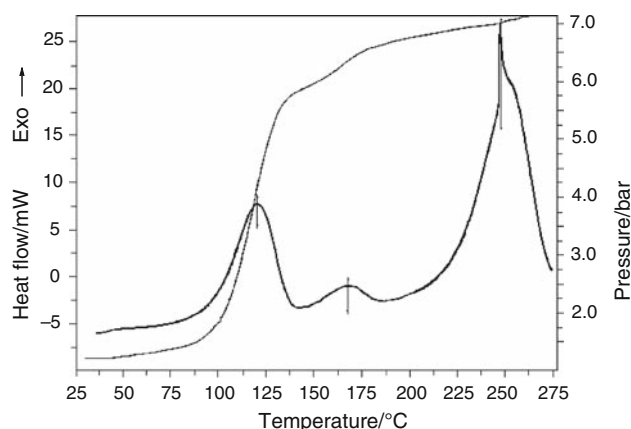


Fig. 6 C80 plot of the TD in glass vessel at heating scan rate $\Phi = 0.3 \text{ °C min}^{-1}$ under nitrogen of the azide **4**

characteristic initial fragmentation (M-28) of the molecular ion at m/z 223 ($M^{+\bullet}$, <3%) leaves a mass spectrum identical to that reported for benzoisoxazole **4a** [41], but which is different than that reported for acridinone **4b**. However, **4b** does display some peaks in the MS that are common to **4a**. The authors suggest a possible thermal partial conversion of **4a** to **4b** via a nitrene intermediate under these conditions may account for these results.

Similarly, the mass spectra of azides **2** and **3** show molecular ions at m/z 147 and 161 ($M^{+\bullet}$, 7 and 3%), respectively, and after the initial fragmentation (M-28) follow overall patterns identical to those reported for the corresponding benzoisoxazoles **2a** and **3a**, respectively [42]. In contrast, the mass spectrum of azide **1** shows a remarkably different profile. Its mass spectrum is typical for a molecule undergoing multiple fragmentations. It has a relatively intense molecular ion peak at m/z 149 ($M^{+\bullet}$, >37%). Some of the other fragments can be attributed to red-ox processes involving the phenyl ring (aniline, 2-aminobenzaldehyde and benzaldehyde), or the extrusion of small molecules (propionitrile, cyclopropylamine, allyl amine), whose formation greatly increases the exothermic peak's magnitude.

It is well known that the controlled decomposition of azide **5** in boiling toluene gives the corresponding benzo[*c*][1,2,5]oxadiazole 1-oxide **5a** in 88% yield [29, 43]. The reaction has been deeply investigated from both the experimental and theoretical [44] points of view, since the reaction produces heterocyclic compounds important in biochemical and pharmacological applications. The MS-EI spectrum of azide **5** at 27 °C again shows the initial molecular ion at m/z 164 with a very low intensity ($M^{+\bullet}$, <5%), which is followed by fragmentation (M-28), and then by an overall pattern identical to that reported for the corresponding benzoxadiazole **5a** [45].

Among the azides under investigation, azide **5** contains the most favourable oxygen balance, which has a clear influence on the heat capacity of its TD when carried out in a closed or open vessel (see Table 2). TG-SDTA-FTIR-MS techniques allow the spectroscopic (IR and MS) characterisation of the thermal process's products and a qualitative understanding of the flux of heat, which is associated with the sample's first weight loss in the DSC profile. As shown in Fig. 7, the sample loses 30% of its weight during the evolution of the first exothermic peak. The C80-FTIR spectrum shows no sign of any IR active gasses, and the mass spectrum indicates the exclusive presence of nitrogen. During the second weight loss at temperatures over 160 °C, an IR spectrum identical to that of the benzo[*c*][1,2,5]oxadiazole 1-oxide **5a** was observed [46]. The identity of this compound was also confirmed using the mass spectrum instrument interfaced directly with the TD vessel.

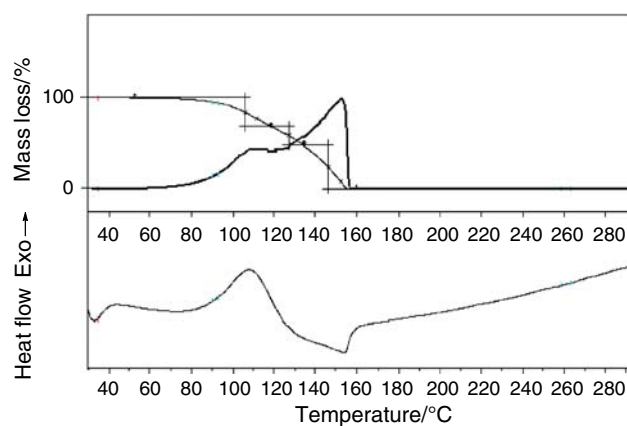


Fig. 7 TG curve (upper) of weight loss, its first derivative and the heat flux measured by SDTA (differential thermal analysis) (lower) for azide **5** undergoing TD between 30 and 300 °C with $\Phi = 5$ °C min⁻¹ under a 60.0 mL min⁻¹ stream of nitrogen

The thermal behaviour of **5** was also investigated by DSC tests ($\Phi = 5$ °C min⁻¹), carried out under both oxidative and inert conditions that consisted of TDs performed in two steps as illustrated in Fig. 8.

The DSC profile was characterised by an initial exothermic peak at $T_p = 121.26$ °C, corresponding to the decomposition of azide **5**. When the vessel was cooled to allow the crystallisation of the resulting product, subsequent heating of the vessel to 300 °C showed an endothermic melting peak at 71 °C for **5a** (lit. mp 71–73 °C [20]) and an exothermic decomposition starting at $T_i = 180.61$ with $T_p = 192.87$. It is noteworthy that the enthalpy of decomposition for azide **5** ($\Delta_d H = -471.5$ J g⁻¹) measured by the C80 under nitrogen, resulted in a value four times smaller than that of the benzo[*c*][1,2,5]oxadiazole 1-oxide (**5a**) ($\Delta_d H = -1953.9$ J g⁻¹). Moreover, the C80 investigation reveals a significant pressure increase of about 20 bars for

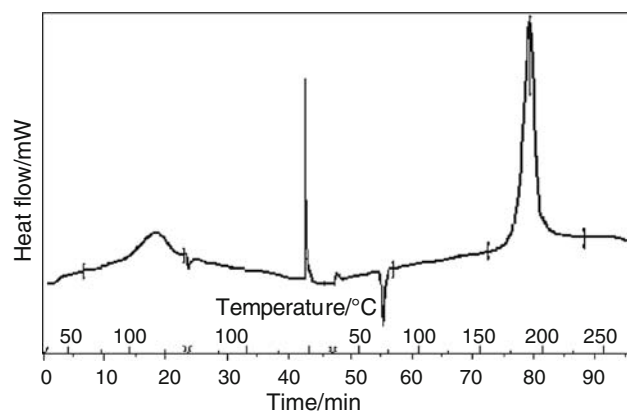
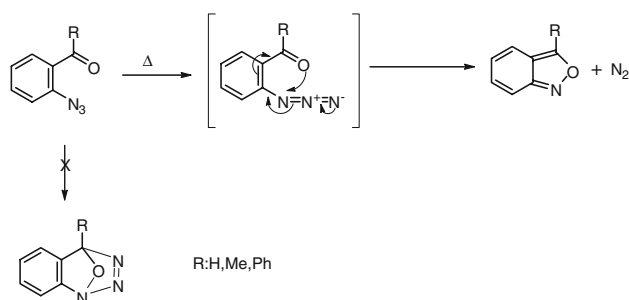


Fig. 8 DSC curve of the probe ($\Phi = 5$ °C min⁻¹) for the product **5a** from the TD of the azide **5**

the entire process. This is associated with **5a**'s highly exothermic enthalpies of decomposition, especially under oxidative conditions, which have been reported to be mainly due to the low dissociation enthalpy of the N–O bond [47, 48]. For most classes of compounds, including organic azides, the primary cleavage represents a qualitative indicator of the stability of a compound and correlates with the ground state energy content, which can be used to compare the relative stabilities of compounds. The investigation of TD mechanisms by computational modelling is important both to gain an appreciation for how energy is stored and released and to gain information useful for the design of more stable molecules. Using density functional theory (DFT) at the B3LYP/6-31G* level [the data were obtained using the standard program Spartan '06 Windows, released by Wavefunction Inc., Irvine, CA (2006) (www.wavefun.com), running on an AMD K7 processor at 1333 MHz], the structures and the energetics of the starting azides **1–5** and the products of the pericyclic reactions (**2a–5a**) were optimised (including the calculation of the LUMO–HOMO gap). Other possible intermediate structures involved in the TD, such as bridged bicyclic structures that would result from potential intramolecular 1,3-cycloadditions, were not considered here (see Scheme 3). In all cases, the energies separating the HOMO and LUMO orbitals ($\Delta E = 1: 5.095$; **2**: 4.709; **3**: 4.764; **4**: 4.481; **5**: 4.350 eV) are in good agreement with the activation energies (E_a) presented and those previously reported, with the slight exception of azide **3**.

A kinetic validation of the TD of azide **3** was carried out using a DSC test performed isothermally at 95 °C for 27 min, which showed an exothermic peak at the same $T_p = 130.83$ °C, but with a heat of decomposition ($\Delta_d H$) twofold smaller than the normal scan (see Fig. 3) due to the partial evaporation of the resulting product. This phenomenon was confirmed by TG-SDTA and C80 experiments that involved warming azide **3** to 140 °C and confirming the formation of 3-methylbenzo[*c*]isoxazole (**3a**) by examining ^1H - and ^{13}C -NMR spectra of the residue.



Scheme 3 Possible mechanism of the TD first step

Conclusions

The potentially dangerous properties and thermo-chemical behaviours of five *ortho*-substituted phenyl azides (**1–5**) were investigated by readily accessible DSC, TG and C80 calorimetric combined with NMR, FTIR and mass spectroscopic techniques. These modern techniques require only small amounts of the compounds to be tested and share the advantages of being highly specific, accurate, clean and versatile. In this case, their application allowed investigations into thermo-chemical transformations, like the pericyclic process that generates benzoxazoles **2a–4a** and benzoxadiazole **5a** in the ‘solid phase’, and into the properties of the starting azides and resulting products. The rate enhancements, low activation energies and negative activation entropies determined for the TD of azides **3** and **4**; which are different from those measured for the azide **1** but were comparable with those previously measured by means of ‘controlled’ thermal reactions in solution. This study confirms the effectiveness of ‘solid phase’ methods for studying thermal processes in a field where the characterisation of the hazardous properties of compounds must be gained and the mechanistic aspect could be considered.

Acknowledgements The authors gratefully acknowledge the ‘Ministero della Università e Ricerca’ for the majority of the financial support for this study, and the Ateneo di Bologna from the ‘Progetto di Finanziamento Triennale’.

References

1. Bayley H, Staros JV. Photoaffinity labelling and related techniques. In: Scriven EFV, editor. Azides and nitrenes, reactivity and utility. Orlando: Academic Press; 1984. p. 433–90.
2. Breslow DS. Industrial application. In: Scriven EFV, editor. Azides and nitrenes, reactivity and utility. Orlando: Academic Press; 1984. p. 491–521.
3. Brase S, Gil C, Knepper K, Zimmermann V. Organic azides: an exploding diversity of a unique class of compounds. *Angew Chem Int Ed Engl.* 2005;44:5188–240.
4. Urben PG, editor. Bretherick’s handbook of reactive chemical hazards, vols 1 and 2. 7th ed. Amsterdam: Elsevier; 2007.
5. Cartwright M, Wilkinson J. New trends in research of energetic materials. In: Ottis J, Pachman J, editors. Proceedings of the Seminar, vol. 1. 11th ed. Czech Republic: Pardubice; 2008. p. 99–112.
6. Huynh M-HV, Hiskey MA, Chavez DE, Naud DL, Gilardi RD. Synthesis, characterization, and energetic properties of diazido heteroaromatic high-nitrogen C–N compound. *J Am Chem Soc.* 2005;127:12537–43.
7. Duddu R, Dave PR, Damavarapu R, Surapaneni R, Gilardi R, Parrish D. Synthesis of azido heterocycles. *Synth Commun.* 2008; 38:767–74.
8. Agrawal JP, Hodgson RD. Organic chemistry of explosives. Chichester: Wiley; 2007. p. 333–9.
9. Walton R, Lahti PM. An efficient, simple synthesis of 4-azido-benzaldehyde. *Synth Commun.* 1998;28:1087–92.

10. Cardillo P, Gigante L, Lunghi A, Fraleoni-Morgera A, Zanirato P. Hazardous N-containing system: thermochemical and computational evaluation of the intrinsic molecular reactivity of some aryl azides and diazides. *New J Chem*. 2008;32:47–53.
11. Salatelli E, Zanirato P. The conversion of furan-, thiophene- and selenophene-2-carbonyl azides into isocyanates: a DSC analysis. *ARKIVOC* 2002;xi:6–16.
12. Stadlbauer W, Hojas G. Study of the thermal behavior of azidoheterenes with differential scanning calorimetry. *J Biochem Biophys Methods*. 2002;53:89–99.
13. Smith PAS. Aryl and heteroaryl azides and nitrenes. In: Scriven EFV, editor. *Azides and nitrenes, reactivity and utility*. Orlando: Academic Press; 1984. p. 95–204.
14. Schuster GB, Platz MS. Photochemistry of phenyl azide. *Adv Photochem*. 1992;17:69–73.
15. Hrovat DA, Waali EE, Thatcher Borden W. Ab initio calculations of the singlet-triplet energy difference in phenylnitrenes. *J Am Chem Soc*. 1992;114:8698–9.
16. Albin A, Bettinetti G, Minoli G. The effect of the p-nitro group on the chemistry of phenylnitrene. A study via intramolecular trapping. *J Chem Soc Perkin*. 1999; 1:2803–7.
17. Kvaschoff D, Bednarek P, George L, Pankajakshan S, Wentrup C. Different behavior of nitrenes and carbenes on photolysis and thermolysis: formation of azirine, ylidic cumulene, and cyclic ketenimine and the rearrangement of 6-phenanthridylcarbene to 9-phenanthrylnitrene. *J Org Chem*. 2005;70:7947–55.
18. Fraleoni-Morgera A, Zanirato P. BF₃·OEt₂-promoted synthesis of acridines via N-aryl nitrenium-BF₃ ions generated by dissociation of 2-oxo azidoarenes in benzene. *ARKIVOC*. 2006;1: 111–20.
19. Dyal LK, Kemp JE. Neighbouring-group participation in pyrolysis of aryl azides. *J Chem Soc B*. 1968; 976–9.
20. Dyal LK, Holmes A-L. Pyrolysis of aryl azides. IX. Azomethines as weak neighboring groups. *Aust J Chem*. 1988;41:1677–86.
21. Hall JH, Behr FE, Reed RL. Cyclization of 2-azidobenzophenones to 3-phenylanthranils. Examples of an intramolecular 1,3-dipolar addition. *J Am Chem Soc*. 1972;94:4952–8.
22. Noelting E, Michel O. Direkte ueberführung von aminen in diazoimide mittels stickstoffwasserstoffsäure. *Chem Ber*. 1893;26: 86–92.
23. Dyal LK. Pyrolysis of aryl azides. VII. Interpretation of Hammett correlations of rates of pyrolysis of substituted 2-nitroazidobenzene. *Aust J Chem*. 1986;39:89–101.
24. Ardakani MA, Smalley RK, Smith RH. 1H- and 2H-indazoles by thermal and photolytic decomposition of o-azidobenzoic acid and o-azidobenzaldehyde derivatives. *J Chem Soc Perkin*. 1983;1: 2501–6.
25. Smolinsky G. Notes—The vapor phase pyrolysis of several substituted azidobenzenes. *J Org Chem*. 1961;26:4108–10.
26. Sakai K, Anselme J-P. Rational synthesis of 2-aminoindazole. *J Org Chem*. 1972;37:2351–2.
27. Meisenheimer J, Senn O, Zimmermann P. Über die oxime des o-amino-benzo- und acetophenons. *Chem Ber B*. 1927;60: 1736–48.
28. Smith PAS, Brown BB, Putney RK, Reinisch RF. The synthesis of heterocyclic compounds from aryl azides. iii. some six-membered rings and some azidobiaryls. *J Am Chem Soc*. 1953;75: 6335–7.
29. Monge A, Palop JA, Lopez de Cerain A, Senador V, Martinez-Crespo FJ, Sainz Y, et al. Hypoxia-selective agents derived from quinoxaline 1,4-di-N-oxides. *J Med Chem*. 1995;38:1786–92.
30. Dyal LK, Kemp JE. The infrared spectra of aryl azides. *Aust J Chem*. 1967;20:1395–402.
31. Von E, Doering W, De Puy CH. Diazocyclopentadiene. *J Am Chem Soc*. 1953;75:5955–7.
32. Boyer JH, Toggweiler U, Stoner GA. Spectrophotometric relationships between furoxanes and nitroso compounds. *J Am Chem Soc*. 1957;79:1748–51.
33. Smith PAS, Hall JH. Kinetic evidence for the formation of azene (electron-deficient nitrogen) intermediates from aryl azides. *J Am Chem Soc*. 1962;84:480–5.
34. Barton DHR, Sammes PG, Weingarten GG. Photochemical transformations. Part XXVIII. Aryl azides as potential photosensitive protecting groups. *J Chem Soc C*. 1971;721–8.
35. Minato M, Lahti PM. Intramolecular exchange coupling of aryl nitrenes by oxygen. *J Phys Org Chem*. 1994;7:495–502.
36. Watson ES, O'Neill MJ, Justin J, Brenner N. A differential scanning calorimeter for quantitative differential thermal analysis. *Anal Chem*. 1964;36:1233–8.
37. Seaton WH. Group contribution method for predicting the potential of a chemical composition to cause an explosion. *J Chem Educ*. 1989;66:A137.
38. Frurip D, Britton L, Fenlon W, Going J, Harison BK, Niemier J, et al. The role of ASTM E27 methods in hazard assessment: Part I. Thermal stability, compatibility, and energy release estimation methods. *Process Saf Prog*. 2004;23:266–78.
39. Cardillo P, Gigante L, Lunghi A, Di Bari C, Ludovisi G. La termodinamica per la sicurezza chimica: criteri di previsione dell'instabilità termica. *Riv Combust*. 2002;56:209–23.
40. Sabbah R, El Watik L. Étude thermodynamique de l'acridone et de la thioxanthone. *Can J Chem*. 1992;70:24–8.
41. Dyal LK, Karpa GJ. Mass spectra of 3-phenyl-2,1-benzisoxazoles. *Org Mass Spectrom*. 1989;24:70–3.
42. Doppler T, Schmid H, Hansen H-J. Zur photochemie von 2, 1-benzisoxazolen (anthranilen) und thermischen und photochemischen umsetzungen von 2-azido-acylbenzolen in stark saurer lösung. *Helv Chim Acta*. 1979;62:271–303.
43. Boulton AJ, Gray ACG, Katritzky AR. Heterocyclic rearrangements. Part. IV, Furoxan- and furazan-benzofuroxan. *J Chem Soc*. 1965;5958–64.
44. Rauhut G, Eckert F. A computational study on the mechanism and kinetics of the pyrolysis of 2-nitrophenyl azide. *J Phys Chem A*. 1999;103:9086–92.
45. Leitão MLP, Pilcher G, Acree WE Jr, Zvaigzne AI, Tucker SA, Ribeiro Da Silva MDMC. Enthalpies of combustion of phenazine N-oxide, phenazine, benzofuroxan, and benzofurazan: the dissociation enthalpies of the (N–O) bonds. *J Chem Thermodyn*. 1990;22:923–8.
46. Gaughran RJ, Picard JP, Kaufman JVR. Contribution to the chemistry of benzofuroxan and benzofurazan derivatives. *J Am Chem Soc*. 1954;76:2233–6.
47. Acree WE Jr, Pilcher G, Ribeiro da Silva MDMC. The dissociation enthalpies of terminal (NO) bonds in organic compounds. *J Phys Chem*. 1982;34:560–2.
48. Zhang C, Shu Y, Huang Y, Zhao X, Dong H. Investigation of correlation between impact sensitivities and nitro group charges in nitro compounds. *J Phys Chem B*. 2005;109:8978–82.